Petroleum Science (2019) 16:32–43
https://doi.org/10.1007/s12182-018-0291-5

ORIGINAL PAPER

Numerical simulation of enhancing coalbed methane recovery by injecting CO_2 with heat injection

Hui-Huang Fang[1,2] · Shu-Xun Sang[1,2] · Shi-Qi Liu[3,4]

Received: 26 December 2017 / Published online: 7 January 2019

Abstract

The technology used to enhance coalbed methane (CBM) recovery by injecting CO_2 (CO_2-ECBM) with heat, combining heat injection with CO_2 injection, is still in its infancy; therefore, theoretical studies of this CO_2-ECBM technology should be perused. First, the coupling equations of the diffusion–adsorption–seepage–heat transfer fields of gas are established. The displacement processes under different pressures and temperatures are simulated by COMSOL. Finally, the displacement effects, a comparison of the CO_2 storage capacity with the CH_4 output and the effective influencing radius of CO_2 injection are analyzed and discussed. The results show that (1) the displacement pressure and temperature are two key factors influencing the CH_4 output and the CO_2 storage capacity, and the increase in the CO_2 storage capacity is more sensitive to temperature and pressure than the CH_4 output. (2) The gas flow direction is from the injection hole to the discharge hole during the displacement process, and the regions with high velocity are concentrated at the injection hole and the discharge hole. (3) A reduction in the CH_4 concentration and an increase in the CO_2 concentration are obvious during the displacement process. (4) The effective influencing radius of injecting CO_2 with heat increases with the increase in time and pressure. The relationship between the effective influencing radius and the injection time of CO_2 has a power exponential function, and there is a linear relationship between the functional coefficient and the injection pressure of CO_2. This numerical simulation study on enhancing CBM recovery by injecting CO_2 with heat can further promote the implementation of CO_2-ECBM project in deep coal seams.

Keywords CO_2-ECBM · Numerical simulation · Displacement effect · COMSOL · CO_2 storage capacity · Effective influencing radius

1 Introduction

Enhancing coalbed methane (CBM) recovery by injecting CO_2 (CO_2-ECBM) is a new technology used to increase CBM production (Pan et al. 2017; Ranathunga et al. 2017a, b), indicating that CO_2 can be permanently sequestered in unmineable coal seams and thus increase CBM production (Li et al. 2017). The adsorption capacity of CO_2 in coal is better than that of CH_4 in high-temperature and pressure environment (Andreas and Yves 2011). Therefore, when CO_2 is injected and adsorbed on a matrix in coal, it can improve not only the CO_2 storage capacity, but also the CH_4 output (Pratama et al. 2018).

The injected CO_2 has a supercritical state and a normal state (Yasunami et al. 2010; Vanelle and Gajewski 2011). Although supercritical CO_2 has excellent enhancement effects on increasing the CH_4 output compared to normal CO_2 (Ranathunga et al. 2017a, b), the requirement for

Edited by Jie Hao

✉ Shu-Xun Sang
shxsang@cumt.edu.cn

1 Key Laboratory of Coalbed Methane Resources and Reservoir Formation Process, Ministry of Education, China University of Mining and Technology, Xuzhou 221008, Jiangsu, China

2 School of Resources and Geosciences, China University of Mining and Technology, Xuzhou 221116, Jiangsu, China

3 Low Carbon Energy Institute, China University of Mining and Technology, Xuzhou 221008, Jiangsu, China

4 The Key Laboratory of Coal-based CO_2 Capture and Geological Storage, Jiangsu Province, China University of Mining and Technology, Xuzhou 221008, Jiangsu, China

normal CO_2 to reach supercritical CO_2 (pressure > 7.38 MPa, temperature > 31.1 °C) is relatively stringent (Zhang et al. 2011a, 2013). Therefore, increasing attention has been paid to the displacement process of enhancing CBM recovery by injecting CO_2 with heat in deep coal seams in geological environments that cannot reach supercritical conditions due to the influence of the thermal environment on the pore structures and adsorption behavior (Mandadige 2017; Feng et al. 2017; Zhang et al. 2017).

The numerical simulation to enhance CBM recovery can be divided into heat injection and gas injection (Wei et al. 2007; Zhou et al. 2013). For heat injection, scholars mainly carry out studies based on the experimental simulation and mainly discuss the influences of heat injection on CH_4 seepage velocity and compare CBM production in thermal or nonthermal environments (Yasunami et al. 2010; Vilarrasa and Rutqvist 2017; Qu et al. 2017). Gas injection simulation is more systematic than heat injection simulation (Vishal et al. 2013; Ma et al. 2017). Scholars mainly focus on analyzing and deriving numerical models (i.e., multi-gas adsorption model, heat transfer model and fluid–solid coupled model; Liu and Smirnov 2008; Vishal et al. 2013; Sun et al. 2016), which have been successfully applied to the numerical software (i.e., COMSOL, COMET and SIMEDWin). Previous studies have shown that the injection of heat and CO_2, individually, into coal can enhance CBM production. However, there are few publications on how to combine heat injection and CO_2 injection. Few people are involved in the field of CO_2 with heat injection, and few scholars have considered using CO_2 as a heat-carrying medium.

To improve theoretical studies on technologies to displace CBM by injecting CO_2 with heat, the coupling equations of gas diffusion–adsorption–seepage–heat transfer fields are established, and the displacement processes at different pressures and temperatures are simulated by COMSOL in this research. The displacement effect, the comparison of the CO_2 storage capacity with CH_4 output and the effective influencing radius of CO_2 injection under different pressures and temperatures are analyzed and discussed. Carrying out the numerical simulation of enhancing CBM recovery by injecting CO_2 with heat under the geological conditions of the Qinshui Basin has important practical value and theoretical significance for promoting the implementation of this technology.

2 Theoretical analysis

In this study, COMSOL software (www.comsol.com), based on the finite element method, was used to carry out the numerical simulation analysis of enhancing CBM recovery by injecting CO_2 with heat (Taheri et al. 2017; Liu et al. 2017a, b). COMSOL has been widely used to solve problems in the geosciences (i.e., element migration, fluid migration and heat transfer), and the widely used partial differential equation module has a strong capability of coupling physical fields (Ni et al. 2017; Ma et al. 2017).

2.1 Governing equations

There are several assumptions applied to establish governing equations (Wei et al. 2007; Vishal et al. 2013): (a) Coal is a dual and isotropic porous medium containing both pores and fractures; (b) there is only CO_2 and CH_4 in the coal seam without water, and the adsorption and desorption of multiple gases is in accordance with the extended Langmuir model; (c) the gas in pore is free, conforming to the ideal gas equation; (d) the migration of gas in pores obeys Fick's law, and the transport of gas in fractures obeys Darcy's law; and (e) there is a mass exchange between the diffusion and percolation processes of gas.

2.1.1 Mass conservation equation for gas diffusion motion

The diffusion motion of CH_4 and CO_2 in coal follows the Fick's diffusion law (Eq. 1; Sampath et al. 2017; Liu et al. 2018).

$$\begin{cases} \frac{\partial C_1}{\partial t} - \nabla \cdot \left(D_1 \nabla C_1\right) = -S_1 \\ \frac{\partial C_2}{\partial t} - \nabla \cdot \left(D_2 \nabla C_2\right) = -S_2 \end{cases} \tag{1}$$

where C_1 and C_2 are the mole concentration of CH_4 and CO_2, D_1 and D_1 are the gas diffusion coefficient of CH_4 and CO_2 and S_1 and S_2 denote the source terms, which reflect the mass exchange between adsorption phase and free phase.

2.1.2 Mass conservation equation of gas seepage motion

According to the basic assumptions, the seepage of CH_4 and CO_2 in coal follows Darcy's law based on the analysis of the mass conservation equation (Eq. 2; Xu et al. 2017; Li et al. 2016; Zhong et al. 2016; Le et al. 2017).

$$\begin{cases} \frac{\varphi M_1}{RT}\frac{\partial P_1}{\partial t} - \nabla \cdot \left(\frac{M_1 K_1 P_1}{RT\mu_1}\nabla\left(P_1 + P_2\right)\right) = S_1 \\ \frac{\varphi M_2}{RT}\frac{\partial P_2}{\partial t} - \nabla \cdot \left(\frac{M_2 K_2 P_2}{RT\mu_2}\nabla\left(P_1 + P_2\right)\right) = S_2 \end{cases} \tag{2}$$

where φ denotes the porosity of coal, M_1 *and* M_2 are the mole mass of CH_4 and CO_2, R is the gas constant, T denotes the gas temperature, P_1 and P_2 represent the pressure of CH_4 and CO_2, K_1 and K_2 are the permeabilities of CH_4 and CO_2,

μ_1 and μ_2 represent the dynamic viscosity of CH_4 and CO_2 and S_1 and S_2 are the source term in the seepage field.

2.1.3 Multi-gas adsorption equations

According to basic assumptions, the adsorption amount of each gas follows the Langmuir equation (Li et al. 2017; Liu et al. 2017a, b) when the pressure balance exists in an adsorption saturation state. The S_1 *and* S_2 in the seepage equation can be derived according to Eq. 3.

$$\begin{cases} S_1 = \left(C_1 - \dfrac{\rho_{1a}\rho_c a_1 b_1 P_1}{(1 + b_1 P_1 + b_2 P_2)} \right) \cdot \tau \\ S_2 = \left(C_2 - \dfrac{\rho_{2a}\rho_c a_2 b_2 P_2}{(1 + b_1 P_1 + b_2 P_2)} \right) \cdot \tau \end{cases} \quad (3)$$

where ρ_c is the density of the coal, ρ_{1a} and ρ_{2a} are the density of CH_4 and CO_2 under standard conditions, a_1 and a_2 are the Langmuir volume parameter of CH_4 and CO_2, b_1 and b_2 are the Langmuir pressure parameter of CH_4 and CO_2 and τ denotes the desorption diffusion coefficient, which reflects the difficulty of desorption of the adsorbed gas and diffusion to the fracture system.

2.1.4 Heat transfer equation

According to basic assumptions, the heat transfer in coal follows the heat transfer equation in a porous medium (Eq. 4; Lin et al. 2017; Wang et al. 2017).

$$\begin{aligned} &\left((1-\varphi)\rho_c C_{c,p} + \varphi C_{mix,p}\right)\frac{\partial T}{\partial t} \\ &- c_{mix,p}\left(\frac{C_1 k_1 + C_2 k_2}{C_1\mu_1 + C_2\mu_2}\right)\nabla p \cdot \nabla T - \nabla \cdot \\ &\left(\left((1-\varphi)\beta_c - \varphi\beta_{mix}\right)\cdot\nabla T\right) = Q_{TS} \end{aligned} \quad (4)$$

where $C_{c,p}$ denotes the specific heat capacity of coal, $C_{mix,p}$ denotes the ratio heat capacity of mixed gas, β_c denotes the thermal conductivity of coal, β_{mix} is the thermal conductivity of mixed gas and Q_{TS} is the source terms in the heat transfer field.

2.1.5 Relationship between porosity, permeability and in situ stress

The process of injecting CO_2 with heat is also affected by the in situ stress environment, which further affects the porosity of coal. The expression is as follows:

$$\phi = \left(\phi_0 - \phi_r\right) \exp\left(\alpha_\phi \overline{\sigma_v}\right) + \phi_r \quad (5)$$

where φ_0 denotes the initial porosity of coal, φ_r denotes the porosity of coal in a high-pressure stress state, α_φ denotes the stress sensitivity coefficient of permeability and σ_v denotes average effective stress. The expression is as follows:

$$\overline{\sigma_v} = \left(\sigma_1 + \sigma_2 + \sigma_3\right)/3 + \alpha P \quad (6)$$

where α denotes the effective stress coefficient of Biot and σ_1, σ_2 and σ_3 denote the minimum, intermediate and maximum principal stress, respectively.

In addition, there is an exponential relationship between permeability and porosity:

$$k = k_0 \exp\left[22.2\left(\phi/\phi_0 - 1\right)\right] \quad (7)$$

where k denotes the permeability after stress action and k_0 denotes the initial permeability.

2.2 Coupling of equations

The processes of enhancing CBM recovery by injecting CO_2 with heat include the processes of gas seepage–adsorption–diffusion–heat transfer in a porous medium. The seepage field, coupled with the diffusion field through flow velocity and with the adsorption field through source terms, is coupled with the heat transfer field by controlling convection heat transfer. The multiple gas adsorption field, coupled with the diffusion field through the concentration distribution and the seepage field through the partial pressure, is coupled with the heat transfer field by the relationship between the adsorption constant and temperature. When the heat transfer field is influenced by the seepage velocity, the temperature distribution will also affect the permeability distribution, gas density and gas viscosity in the seepage field. Meanwhile, it will also affect the adsorption constant in the adsorption field, so that it can be coupled with the multiple gas adsorption field. The porosity and permeability will also be affected by the in situ stress environment.

3 Model description and model validation against experimental data

3.1 Model description

The process of enhancing CBM recovery by injecting CO_2 and heat is a three-dimensional process that can be simplified to a two-dimensional (2D) process by considering the feasibility and effectiveness of numerical calculation (Sang et al. 2016). The geological model is a square area of 20 m, one-fourth region of which is selected as the numerical simulation area considering the symmetry of the affected area (Fig. 1). The upper right corner of the region is the CO_2 injection hole (H_{in}), and the lower left corner is the CH_4

discharge hole (H_{out}). The centerline, L, connecting the CO_2 injection hole and the CH_4 discharge hole, is selected as a 2D transversal (Fig. 1).

3.2 Simulation schemes and physical parameters

To explore the stimulation effect of enhancing CBM recovery by injecting CO_2 with heat, the simulation schemes can be carried out as follows (Table 1). By changing the injection pressure or temperature, this paper carries out a comparative study of displacement effect with different displacement pressures at the same injection temperature and different injection temperatures at the same displacement pressure.

The TL-003 well concerning the CO_2-ECBM process in the southern Qinshui Basin is the first technical well in China (Zhang et al. 2011b). For the numerical simulation of enhancing CBM recovery by injecting CO_2 and heat, all parameters concerning coal are derived from the experimental results of the same samples collected from No. 3 coal seams in the TL-003 well (i.e., mercury injection experiments, liquid nitrogen experiment, adsorption experiments, nuclear magnetic resonance and displacement experiment). Other parameters needed for the numerical simulation are derived from other scholars' research results in the same research area (Ye et al. 2007, 2012, 2016). The relevant parameters are given in Table 2.

3.3 Boundary setting and initial conditions

3.3.1 Seepage field

According to the simulation scheme, the boundary condition of the CO_2 injection hole is constant pressure, and the p_{in} is 3 MPa, 5 MPa and 7 MPa, respectively. The boundary condition of the CH_4 discharge hole is connected to the bottom hole flow pressure; thus, the p_{out} is set to 0.5 MPa. The condition of the other boundaries is set to zero flow. It is assumed that the initial pressure of the coal seams is 2.5 MPa, the free gas pressure is 2.5 MPa, and the adsorbed gas is a saturated adsorption state at 2.5 MPa.

3.3.2 Diffusion field

According to the simulation scheme, the boundary condition of the CO_2 injection hole is a constant concentration, and the concentration of CO_2 is 820 mol/m^3, 1641 mol/m^3 and 2462 mol/m^3, respectively. The boundary condition of the CH_4 discharge hole is connected to the export. The condition of the other boundaries is set to zero flow. It is assumed that CH_4 at a concentration of 451.7 mol/m^3 in the coal is saturated at 2.5 MPa in the original condition, and there is no CO_2 in the coal.

Table 1 Numerical simulation scheme of enhancing CBM recovery by injecting CO_2 with heat

Injection pressure, MPa	Injection temperature, K
3	293.15
5	293.15
7	293.15
5	313.15
5	333.15

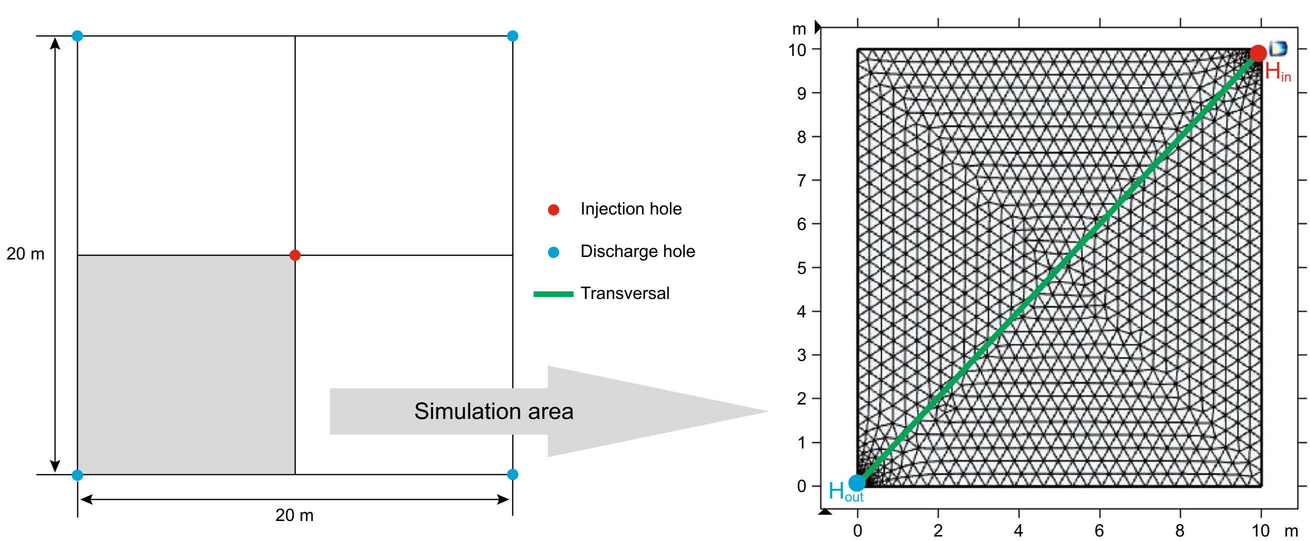

Fig. 1 Geological model of enhancing CBM recovery by injecting CO_2 with heat injection

Table 2 Physical parameters of numerical simulation for enhancing CBM recovery by injecting CO_2 with heat injection

Symbol	Parameter	Value	Unit
ρ_c	Density of coal	1.38×10^3	kg/m^3
φ_0	Initial porosity of coal	0.084	–
k_0	Initial permeability of coal	2.6×10^{-16}	m^2
M_1	Mole mass of CH_4	16	g/mol
a_1	Langmuir parameter of CH_4	0.03832	m^3/kg
b_1	Langmuir parameter of CH_4	0.51	1/MPa
μ_1	Dynamic viscosity of CH_4	1.03×10^{-5}	Pa s
M_2	Mole mass of CO_2	44	g/mol
a_2	Langmuir parameter of CO_2	0.06329	m^3/kg
b_2	Langmuir parameter of CO_2	1.92	1/MPa
μ_2	Dynamic viscosity of CO_2	1.38×10^{-5}	Pa S
R	Gas constant	8.314	J/(mol K)
β_c	Thermal conductivity of coal	0.2	W/(m K)
$C_{c,p}$	Specific heat capacity of coal	1.25×10^3	J/(kg K)
α_φ	Stress sensitivity coefficient of permeability	5.0×10^{-8}	Pa^{-1}
α	Effective stress coefficient of Biot	1	–
τ	Desorption diffusion coefficient	1.42	ms

3.3.3 Heat transfer field in a porous medium

According to the simulation scheme, the boundary condition of the CO_2 injection hole is a constant temperature, and the T_{in} is 293.15 K, 313.15 K or 333.15 K, respectively. The boundary condition of the CH_4 discharge hole is connected with the atmosphere. It is defined as the constant temperature boundary, and the T_{out} is 293.15 K. The condition of the other boundaries is set to a constant temperature. It is assumed that the initial temperature of the coal seam is 293.15 K.

3.4 Model validation against experimental data

Some laboratory experiments can be carried out to verify the accuracy of the coupling models. The setting of the required parameters and boundary conditions are consistent with the numerical simulation conditions. The laboratory experiments maintain the isothermal process, which means that the displacement mole fraction of CO_2 (i.e., injection of CO_2 mol number/initial CH_4 mol number) and the displacement efficiency of CH_4 (i.e., output of CH_4 mol number/initial CH_4 mol number) in the numerical simulation results can be better compared to those in the laboratory experiment results without considering the influence of temperature.

Figure 2 shows that the simulation results are in good agreement with the experimental results. With the injection of CO_2, a large amount of CH_4 was displaced from the coal seam, and CO_2 was sequestered in the coal seam. At the initial stage of CO_2 injection, the output rate of CH_4 was high. With the continuous injection of CO_2, the permeability of the coal seam decreased as a result of the adsorption deformation of coal, and the injectivity of CO_2 was reduced. It can also be seen that the experimental and simulation results are consistent. The maximum error is less than 10%, which proves the rationality of the coupling models by injecting CO_2. Therefore, the coupling models with multi-physical fields can be used to simulate the displacement process by injecting CO_2 with a heat injection.

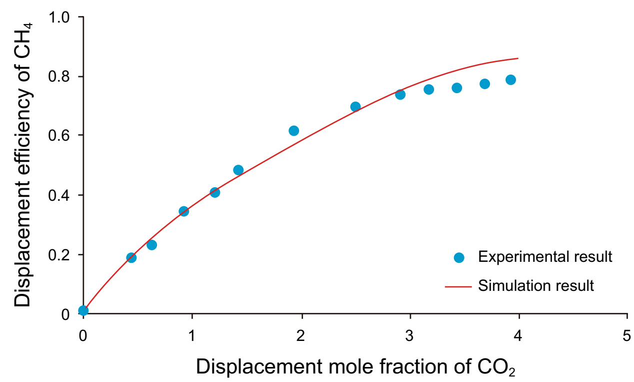

Fig. 2 Comparison of the experimental results and the simulation results for displacement efficiency

4 Results and analysis

In this study, the displacement effect of enhancing CBM recovery by injecting heat and CO_2 can be analyzed from gas injection, different displacement pressures and different displacement temperatures.

4.1 Displacement process of gas injection and the analysis of this effect

The displacement effect of gas injection can be analyzed according to the pressure distribution, the temperature distribution and the concentration distribution.

Figure 3 shows that CO_2 at high pressure moves from the CO_2 injection hole toward the middle of the coal seam as time goes on. On the 10th day, the pressure distribution reached 7 m. On the 50th day, the influencing range of gas pressure has nearly covered the entire coal seam. The gas pressure in coal changes obviously when the time of the gas injection lasts for less than 40 days. The gas pressure changes slowly as the displacement time increases, especially after the 60th day. The partial pressure of CH_4 increases due to the energy caused by CO_2. The highest point of the pressure moves to the CH_4 discharge hole based on the fact that the injection pressure of CO_2 is higher than that of CH_4 in the original formation.

Although there are convective heat transfer and solid heat transfer in coal, the heat transfer process is very slow, and the ranging radius of temperature is only approximately 7–8 m on the 100th day during the CO_2 injection process (Fig. 4). In the early stage of CO_2 injection, the ranging radius of the temperature obviously changes, but the increase in the radius decreases.

In the simulated period, the CH_4 concentration around the injection hole varies significantly. The reducing range of concentration increases as time passes, and there is an area with a CH_4 concentration near 0 mol/m^3. The influencing radius of CO_2 concentration expands, which is in accordance with the changing range of CH_4 concentration. Therefore, it

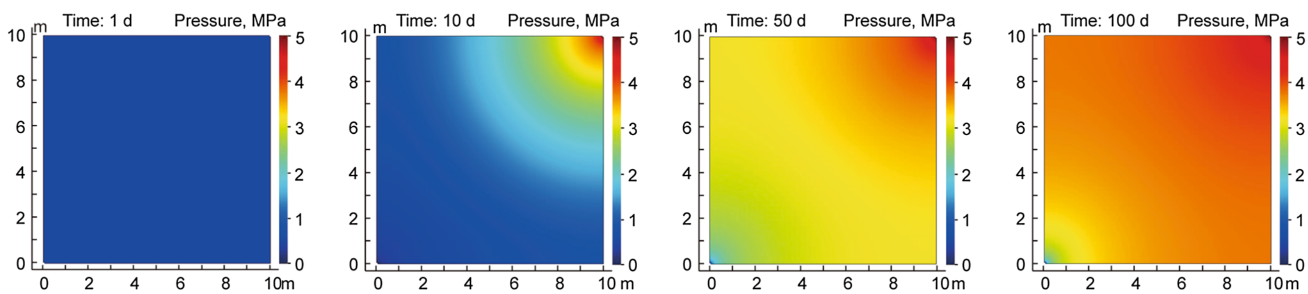

Fig. 3 Pressure distribution during the process of enhancing CBM recovery by injecting CO_2 and heat (at 5 MPa and 313.15 K)

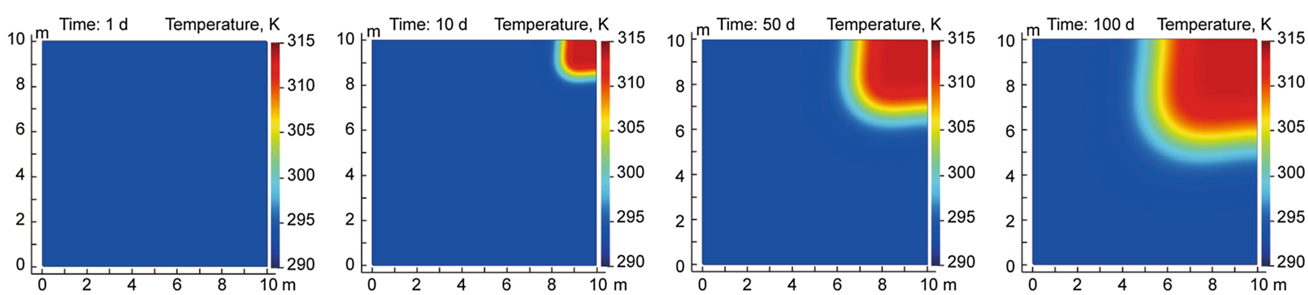

Fig. 4 Temperature distribution of the process of enhancing CBM recovery by injecting CO_2 and heat (at 5 MPa and 313.15 K)

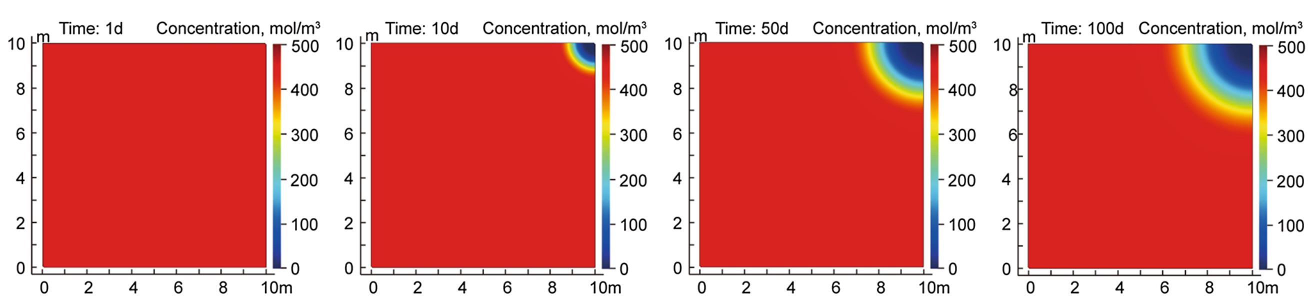

Fig. 5 Concentration distribution of CH_4 regarding enhancing CBM recovery by injecting CO_2 with heat injection (under 5 MPa and 313.15 K)

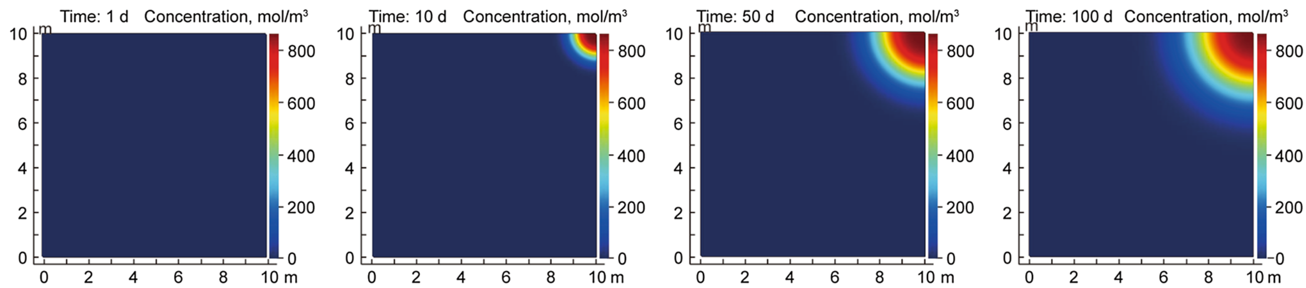

Fig. 6 Concentration distribution of CO_2 regarding enhancing CBM recovery by injecting CO_2 with heat injection (under 5 MPa and 313.15 K)

can be seen that the CO_2 injection has a significant effect on the displacement of CH_4 in coal (Figs. 5, 6). The changing range of CH_4 and the CO_2 concentration has a strong correspondence. The lowest concentration of CH_4 can reach 0 mol/m^3, that is, CH_4 has been completely displaced. The highest concentration of CO_2 can reach 1750 mol/m^3, which shows that coal has a strong carbon sequestration capacity.

4.2 Analysis of the displacement effect under different displacement pressures

The displacement effect under different displacement pressures can be analyzed according to gas pressure and concentration distribution with the same displacement time.

In the same displacement time, the increase in the displacement pressure leads to an obvious change in the gas pressure distribution in coal. Specifically, in the early stage of CO_2 injection, the increase in the displacement pressure can increase the gas pressure in coal over a short time (Fig. 7), which improves the gas energy in the coal seam and allows CH_4 to be easily produced.

At the same time, the greater the displacement pressure is, the larger the range of CH_4 being driven out of coal is (Fig. 8), which shows that the increase in the displacement pressure can effectively remove the CH_4 from the original position and leave the coal seam in a short time, thus improving the CBM production. The greater the displacement pressure is, the greater the migration range of CO_2 in the same time is, and the difference of the influencing scope increases with time (Fig. 9). It is indicated that increasing displacement pressure can store more CO_2 in coal at the same time.

4.3 Analysis of the displacement effect under different displacement temperatures

The displacement effect analysis under different temperatures is mainly based on temperature distribution in the same displacement time.

In the same displacement time, the higher the injection temperature is, the greater the temperature range is in coal (Fig. 10). Due to the low migration velocity of gas and thermal conductivity of coal, there is little difference between the convection heat transfer and solid heat transfer of coal. Therefore, the temperature difference in coal is not significant for the two cases of displacement temperature of 313.15 K and 333.15 K.

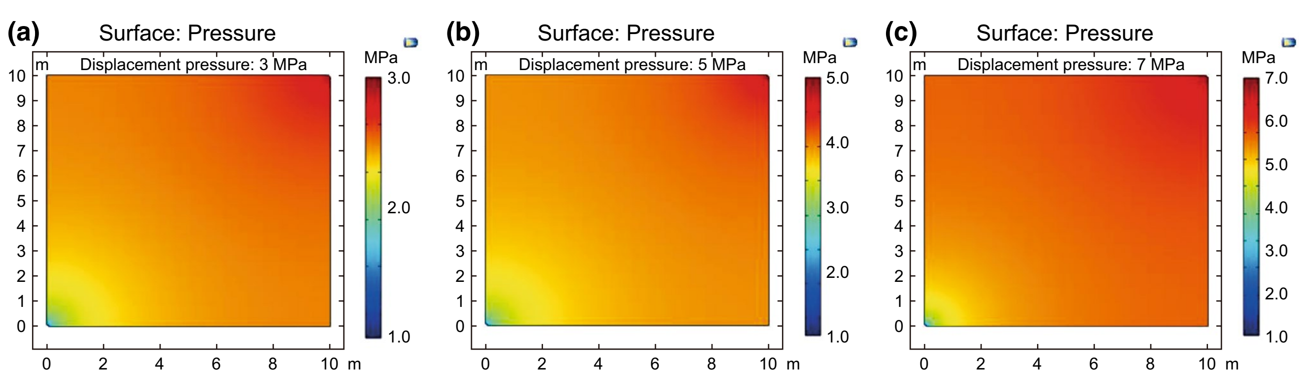

Fig. 7 Distribution of pressure on the 50th day in the coalbed with different displacement pressures: **a** 3 MPa, **b** 5 MPa, **c** 7 MPa

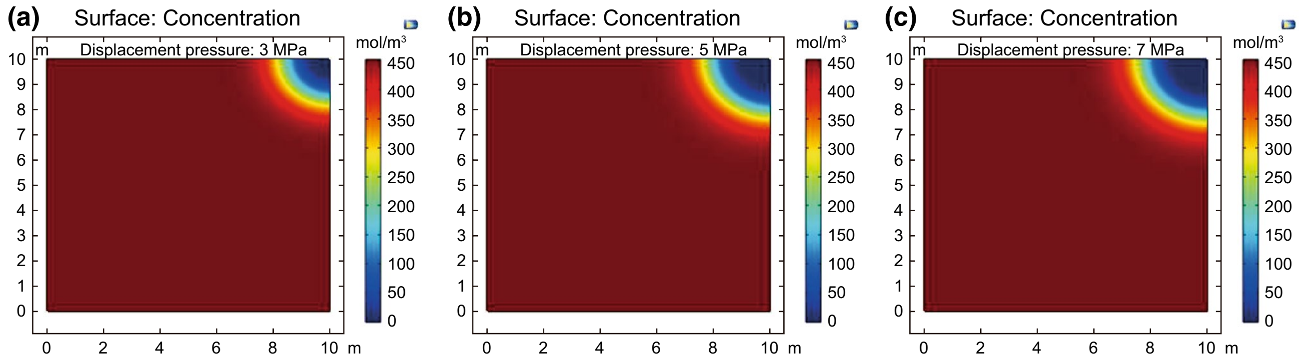

Fig. 8 Concentration distribution of CH_4 on the 50th day in the coalbed with different displacement pressures: **a** 3 MPa, **b** 5 MPa, **c** 7 MPa

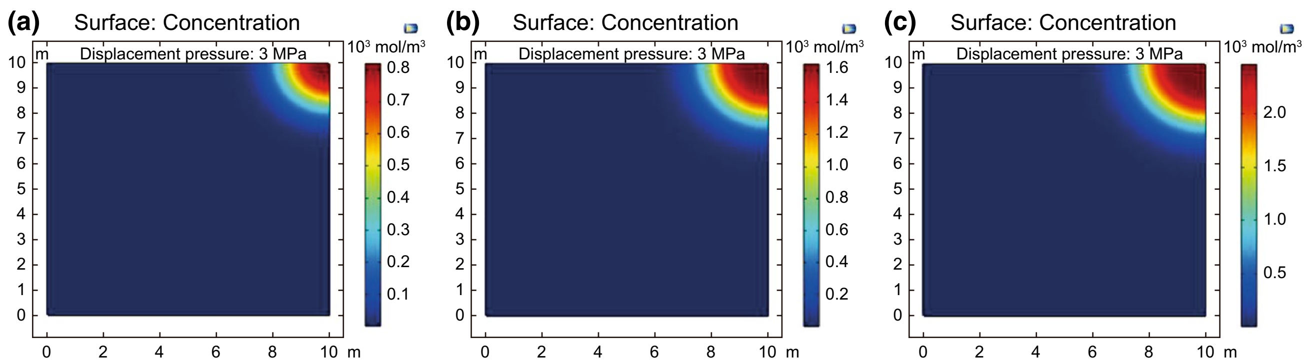

Fig. 9 Concentration distribution of CO_2 on the 50th day in the coalbed with different displacement pressures: **a** 3 MPa, **b** 5 MPa, **c** 7 MPa

5 Discussions

5.1 Comparative analysis of CO_2 storage capacity and CH_4 output

CO_2 storage capacity and CH_4 output increase as time passes within the simulating timescale. With the increase in displacement pressure, there is a significant difference between the CO_2 storage capacity and the CH_4 output (Fig. 11a). When displacement pressure increases from 3 MPa to 7 MPa, the CH_4 output and the CO_2 storage capacity increase from 753.36 mol and 1610.78 mol to 2250.31 mol and 15,032.29 mol, respectively. On the 100th day, the CH_4 output and the CO_2 storage capacity at the displacement pressure of 5 MPa and 7 MPa are 2.00 times, 2.99 times and 4.21 times, 9.33 times that of 3 MPa (Fig. 11a). The displacement ratio is 2.14, 4.49 and 6.69, respectively, when displacement pressure is 3 MPa, 5 MPa and 7 MPa, which shows that the increase in displacement pressure can increase not only the CH_4 output and the CO_2 storage capacity but also the displacement ratio.

There is also a difference between the CH_4 output and the CO_2 storage capacity under different displacement temperatures. With the increase in the displacement temperature, the CH_4 output and the CO_2 storage capacity increase from 1638.32 mol and 6751.13 mol to 1732.11 mol and 6832.32 mol, respectively, on the 100th day. It can be seen that the increase in displacement temperature can increase the CH_4 output and the CO_2 storage capacity at the same time. The increase in the CO_2 storage capacity is more sensitive to temperature than the CH_4 output (Fig. 11b).

The increase in the displacement pressure increases the activation energy of the surface for the matrix in the coal during the displacing process. CO_2 has more contact collisions with CH_4 and will produce more CH_4. The increase in temperature plays a significant role in activating the gas. By heating the coal, the CH_4 adsorbed on the coal surface is more easily desorbed, which moves more CH_4 away from the matrix surface in the coal and provides more adsorption sites for CO_2. Because of the increase in temperature, the coal will produce a new fracture structure due to thermal action, which makes more CO_2 adsorption space in coal. The above aspects cause an increase in the CO_2 volume stored in coal, and the difference between the CH_4 output and the CO_2 storage capacity will become small as the temperature increases. Analyzing the relationship between CH_4 output,

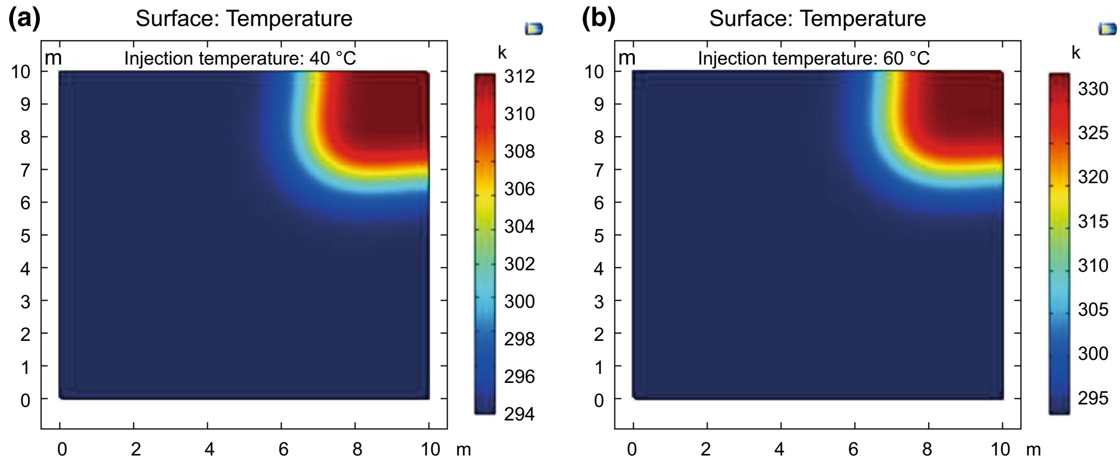

Fig. 10 Temperature distribution in the coal seam on the 50th day with different injection temperatures: **a** 313.15 K, **b** 333.15 K

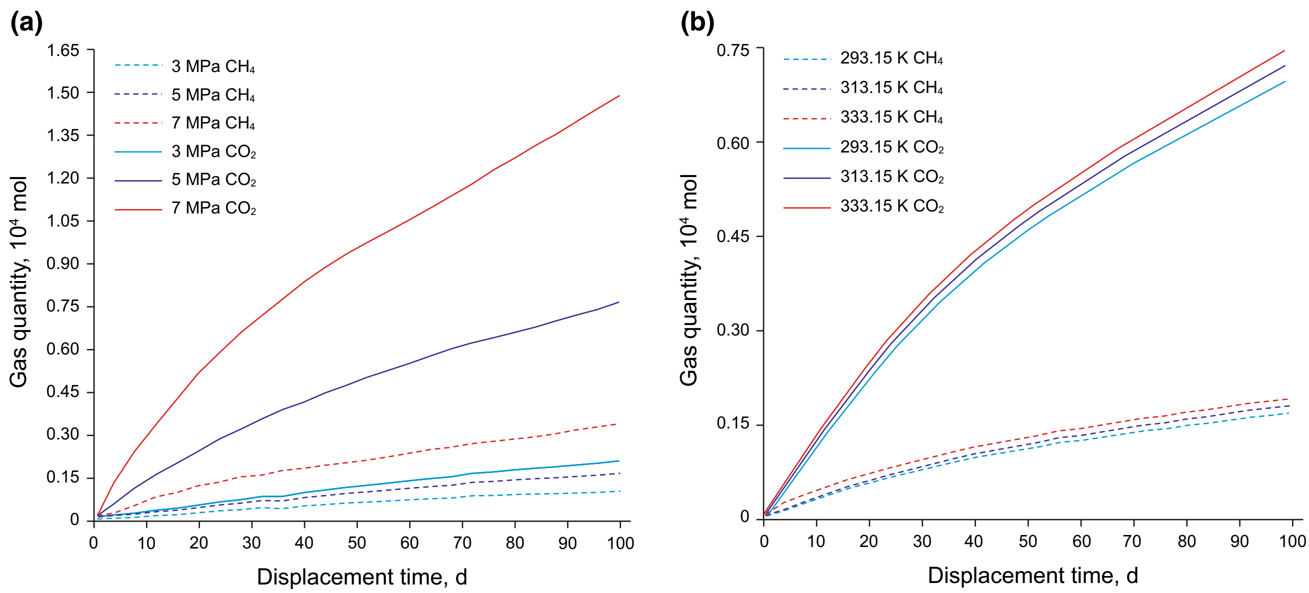

Fig. 11 Distribution diagram of the CH_4 output and the CO_2 storage capacity with time: **a** different displacement pressures and **b** different displacement temperatures

CO_2 storage capacity and time, temperature and pressure of gas injection can guide the development and implementation of the CO_2-ECBM project.

5.2 Analysis of the effective influencing radius of gas injection

The effective influencing radius of gas injection refers to the distance between the point with the lowest effective pressure, which can effectively displace the CH_4 in coal, and the CO_2 injection hole. The minimum distance that conforms to the condition is the effective influencing radius of gas injection (Wang et al. 2012). The author proposes that the radial distance between the point when the CH_4 pressure is reduced to 0.1 MPa in coal and the CO_2 injection hole is the effective influencing radius of the gas injection during the gas injection.

The former analysis shows that when the injection time is longer than 10 days, the effective radius under each injection pressure is greater than that in the simulation area, which is not conducive to the analysis of the effective radius of enhancing CBM recovery by injecting CO_2 with heat injection. Therefore, the first 10 days are chosen to analyze the effective influencing radius of enhancing CBM recovery by injecting CO_2 with heat injection with different injection pressures and times. Table 3 shows that the effective influencing radius of gas injection increases with the increase in

Table 3 Effective influencing radius of enhancing CBM recovery by injecting CO_2 with heat injection with different injection pressures and injection times

Injection time, days	Effective influencing radius with different injection pressures, m		
	3 MPa	5 MPa	7 MPa
1	1.0	1.9	2.9
2	1.8	3.1	4.4
4	2.5	4.4	5.6
6	3.1	5.7	6.3
8	3.6	6.4	7.0
10	4.0	6.9	7.6

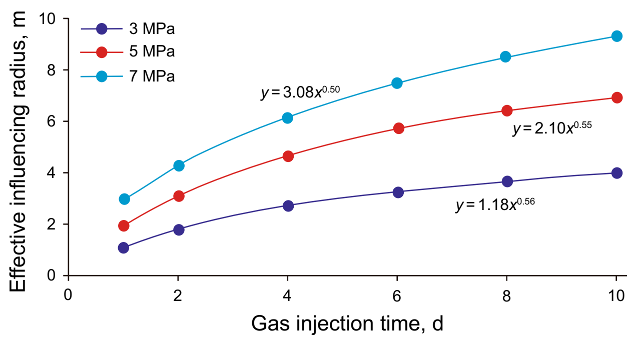

Fig. 12 Relationship between the effective influencing radius and the injection time under different injection pressures

injection time and injection pressure, the increase in which is gradually reduced.

Figure 12 shows that the effective influencing radius increases with the increase in the gas injection time under the same gas injection pressure, and there is an exponential function relationship between the effective influencing radius, R, and the gas injection time, t, $R=At^B$. According to regression analysis, there is a linear relationship among the coefficients, A and B, and the gas injection pressure, P (Fig. 13), where $A=0.47P+0.22$, $B=-0.02P+0.63$ and $R=(0.47P+0.22)t^{(-0.02P+0.63)}$ ($3\leq P\leq 7$ MPa). Analyzing the relationships among the effective influencing radius of gas injection and the gas injection pressure and time, it is beneficial to guide the development and implementation of the CO_2-ECBM project.

6 Conclusion

In this paper, to perfect theoretical studies on the technology to displace CBM by injecting CO_2 with heat injection, the coupling equations of gas diffusion–adsorption–seepage–heat transfer fields are established, and the displacement

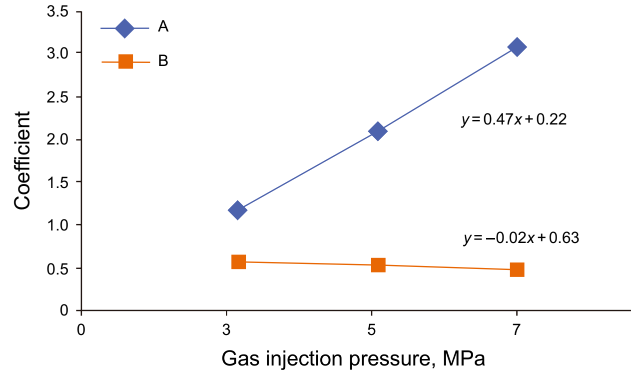

Fig. 13 Relationship between coefficient A and coefficient B and gas injection pressure P

processes under different pressures and temperatures are simulated by COMSOL. The displacement effect, the comparison of the CO_2 storage capacity with the CH_4 output, and the effective influencing radius of CO_2 injection under different pressures and temperatures are emphatically analyzed and discussed. The main conclusions are as follows.

(1) The displacement pressure and temperature are the key factors influencing the CH_4 output and the CO_2 storage capacity, which can be significantly increased by improving the displacement pressure and temperature. The displacement ratio can also be improved. The CO_2 storage capacity is more sensitive to temperature and pressure than the CH_4 output.
(2) The decrease in the CH_4 concentration and the increase in the CO_2 concentration are obvious during the displacement process of injecting CO_2 with heat injection. The coal seams have a high storage capacity for CO_2, and the increase in the displacement radius decreases as time passes.
(3) The effective influencing radius of injecting CO_2 with heat injection is increased with the increase in time and pressure, but the increase in the radius is gradually reduced. The relationship between the effective influencing radius and the time of gas injection has a power exponential function, and there is a linear relationship between the function coefficient and the gas injection pressure. It is beneficial to guide the development and implementation of the CO_2-ECBM project by analyzing the relationship between the effective influencing radius and injection pressure with injection time.

Acknowledgements We would like to express our gratitude to the two anonymous reviewers for offering their constructive suggestions and comments which improved this manuscript in many aspects. The work was financially supported by the National Natural Science Foundation of China (No. 41330638).

References

Andreas B, Yves G. CBM and CO_2-ECBM related sorption processes in coal: a review. Int J Coal Geol. 2011;87(2):49–71. https://doi.org/10.1016/j.coal.2011.04.011.

Feng GR, Wu YG, Zhang C, Hu S, Shao H, Xu G, et al. Changes on the low-temperature oxidation characteristics of coal after CO_2 adsorption: a case study. J Loss Prevent Proc. 2017;49:536–44. https://doi.org/10.1016/j.jlp.2017.05.018.

Le TD, Murad MA, Pereira PA. A new matrix/fracture multiscale coupled model for flow in shale-gas reservoirs. SPE J. 2017;22(1):265–88. https://doi.org/10.2118/181750-PA.

Li B, Zhao LC, Wang L, Liu C, McAdam KG, Wang B. Gas-phase pressure and flow velocity fields inside a burning cigarette during a puff. Thermochim Acta. 2016;623:22–8. https://doi.org/10.1016/j.tca.2015.11.006.

Li W, Liu HF, Song XF. Influence of fluid exposure on surface chemistry and pore-fracture morphology of various rank coals: implications for methane recovery and CO_2 storage. Energy Fuel. 2017;31(11):12552–69. https://doi.org/10.1021/acs.energyfuels.7b02483.

Lin BQ, Li H, Chen ZW, Zheng C, Hong Y, Wang Z. Sensitivity analysis on the microwave heating of coal: a coupled electromagnetic and heat transfer model. Appl Therm Eng. 2017;126:949–62. https://doi.org/10.1016/j.applthermaleng.2017.08.012.

Liu GX, Smirnov AV. Modeling of carbon sequestration in coalbeds: a variable saturated simulation. Energy Convers Manag. 2008;49(10):2849–58. https://doi.org/10.1016/j.enconman.2008.03.007.

Liu T, Lin BQ, Yang W, Liu T, Kong J, Huang Z, et al. Dynamic diffusion-based multifield coupling model for gas drainage. J Nat Gas Sci Eng. 2017a;44:233–49. https://doi.org/10.1016/j.jngse.2017.04.026.

Liu ZD, Cheng YP, Liu QQ, Jiang JY, Li W, Zhang KZ. Numerical assessment of CMM drainage in the remote unloaded coal body: insights of geostress–relief gas migration and coal permeability. J Nat Gas Sci Eng. 2017b;45:487–501. https://doi.org/10.1016/j.jngse.2017.06.017.

Liu P, Qin YP, Liu SM, Hao YJ. Non-linear gas desorption and transport behavior in coal matrix: experiments and numerical modeling. Fuel. 2018;214:1–13. https://doi.org/10.1016/j.fuel.2017.10.120.

Ma TR, Rutqvist J, Oldenburg CM, Liu WQ. Coupled thermal–hydrological–mechanical modeling of CO_2-enhanced coalbed methane recovery. Int J Coal Geol. 2017;179(15):81–91. https://doi.org/10.1016/j.coal.2017.05.013.

Mandadige SAP. Influences of CO_2 injection into deep coal seams: a review. Energy Fuel. 2017;31(10):10324–34. https://doi.org/10.1021/acs.energyfuels.7b01740.

Ni XM, Miao J, Lv RS, Lin XY. Quantitative 3D spatial characterization and flow simulation of coal macropores based on CT technology. Fuel. 2017;200:199–207. https://doi.org/10.1016/j.fuel.2017.03.068.

Pan ZJ, Ye JP, Zhou FB, Tan YL, Connell LD, Fan JJ. CO_2 storage in coal to enhance coalbed methane recovery: a review of field experiments in China. Fuel Int Geol Rev. 2017;60(4):1–23. https://doi.org/10.1080/00206814.2017.1373607.

Pratama E, Ismail MS, Ridha S. Identification of coal seams suitability for carbon dioxide sequestration with enhanced coalbed methane recovery: a case study in South Sumatera Basin, Indonesia. Clean Technol Environ. 2018;20(3):581–7. https://doi.org/10.1007/s10098-017-1383-4.

Qu HY, Liu JS, Pan ZJ, Peng Y, Zhou F. Simulation of coal permeability under non-isothermal CO_2 injection. Int J Oil Gas Coal T. 2017;15(2):190–215. https://doi.org/10.1504/IJOGCT.2017.10004656.

Ranathunga AS, Perera MSA, Ranjith PG, Wei CH. An experimental investigation of applicability of CO_2 enhanced coal bed methane recovery to low rank coal. Fuel. 2017a;189:391–9. https://doi.org/10.1016/j.fuel.2016.10.116.

Ranathunga AS, Perera MSA, Ranjith PG, Zhang XG, Wu B. Supercritical carbon dioxide flow behaviour in low rank coal: a meso-scale experimental study. J CO2 Util. 2017b;20:1–13. https://doi.org/10.1016/j.jcou.2017.04.010.

Sampath KHSM, Perera MSA, Ranjith PG, Matthai SK, Rathnaweera T, Zhang G, et al. CH_4–CO_2 gas exchange and supercritical CO_2 based hydraulic fracturing as CBM production-accelerating techniques: a review. J CO2 Util. 2017;22:212–30. https://doi.org/10.1016/j.jcou.2017.10.004.

Sang GJ, Elsworth D, Miao XX, Mao XB, Wang JH. Numerical study of a stress dependent triple porosity model for shale gas reservoirs accommodating gas diffusion in kerogen. J Nat Gas Sci Eng. 2016;32:423–38. https://doi.org/10.1016/j.jngse.2016.04.044.

Sun XF, Zhang YY, Li K, Gai ZY. A new mathematical simulation model for gas injection enhanced coalbed methane recovery. Fuel. 2016;183:478–88. https://doi.org/10.1016/j.fuel.2016.06.082.

Taheri A, Sereshki F, Ardejani FD, Mirzaghorbanali A. Simulation of macerals effects on methane emission during gas drainage in coal mines. Fuel. 2017;210:659–65. https://doi.org/10.1016/j.fuel.2017.08.081.

Vanelle C, Gajewski D. Experimental evaluation of permeability of coal in supercritical CO_2 and N_2 injection under stress and strain restricted conditions. Geophys Prospect. 2011;126(10/11):614–22. https://doi.org/10.2473/journalofmmij.126.614.

Vilarrasa V, Rutqvist J. Thermal effects on geologic carbon storage. Earth Sci Rev. 2017;165:245–56. https://doi.org/10.1016/j.earscirev.2016.12.011.

Vishal V, Sing L, Pradhan SP, Singh TN, Ranjith PG. Numerical modeling of Gondwana coal seams in India as coalbed methane reservoirs substituted for carbon dioxide sequestration. Energy. 2013;49(49):384–94. https://doi.org/10.1016/j.energy.2012.09.045.

Wang ZF, Chen JC, Yang HM. Study on effective influence radius of borehole air injection to remove and replace coal bed methane in seam. Coal Sci Technol. 2012;40(9):28–31 **(in Chinese)**.

Wang JL, Lian WH, Li P, Zhang ZL, Yang JX, Hao XG, et al. Simulation of pyrolysis in low rank coal particle by using DAEM kinetics model: reaction behavior and heat transfer. Fuel. 2017;207:126–35. https://doi.org/10.1016/j.fuel.2017.06.078.

Wei XR, Wang GX, Massarotto P, Golding SD, Rudolph V. Numerical simulation of multicomponent gas diffusion and flow in coals for CO_2 enhanced coalbed methane recovery. Chem Eng Sci. 2007;62(16):4193–203. https://doi.org/10.1016/j.ces.2007.04.032.

Xu P, Tie Y, Wang XM. Fluid-solid coupling dynamic equations considering gas desorption contraction and coal motion deformations. Mechanika. 2017;23(3):391–6. https://doi.org/10.5755/j01.mech.23.3.18480.

Yasunami T, Sasaki K, Sugai Y. CO_2 Temperature prediction in injection tubing considering supercritical condition at Yubari ECBM pilot-test. J Can Pet Technol. 2010;49(4):44–50. https://doi.org/10.2118/136684-PA.

Ye JP, Feng SL, Fang ZQ, Wang G, Gunter WD, Wong S, et al. Micro-pilot test for enhanced coalbed methane recovery by injecting carbon dioxide in south part of Qinshui Basin. Acta Petrolei Sinica. 2007;28(4):77–80 **(in Chinese)**.

Ye JP, Zhang B, Sam W. Test and evaluation on elevation of coalbed methane recovery ratio by injecting and burying CO_2 for 3# coal seam of north section of Shizhuang, Qingshui Basin, Shanxi. Chin Acad Eng. 2012;14(2):38–44 **(in Chinese)**.

Ye JP, Zhang B, Han XT, Zhang CJ. Well group carbon dioxide injection for enhanced coalbed methane recovery and key parameter of the numerical simulation and application in deep coalbed methane. J China Coal Soc. 2016;41(1):149–55 **(in Chinese)**.

Zhang SH, Tang SH, Pan ZJ, Shang DZ, Li ZC, Zhang JP. Numerical simulation of CO_2 enhanced coalbed methane recovery on Jincheng anthracite coal reservoir. J China Coal Soc. 2011a;36(10):1741–7 **(in Chinese)**.

Zhang DF, Cui YJ, Liu B, Li SG, Song WL, Lin WG. Supercritical pure methane and CO_2 adsorption on various rank coals of china: experiments and modeling. Energy Fuel. 2011b;25(4):1891–9. https://doi.org/10.1021/ef101149d.

Zhang DF, Gu LL, Li SG, Lian PC, Tao J. Interactions of supercritical CO_2 with coal. Energy Fuel. 2013;27(1):387–93. https://doi.org/10.1021/ef301191p.

Zhang L, Li X, Zhang Y, Cui GD, Tan CY, Ren SR. CO_2 injection for geothermal development associated with EGR and geological storage in depleted high-temperature gas reservoirs. Energy. 2017;123:139–48. https://doi.org/10.1016/j.energy.2017.01.135.

Zhong HB, Liang SR, Zhang JT, Zhu YQ. Multi-fluid model with variable particle density and diameter based on mass conservation at the particle scale. Powder Technol. 2016;294:43–54. https://doi.org/10.1016/j.powtec.2016.02.024.

Zhou FD, Hussain FQ, Cinar Y. Injecting pure N_2 and CO_2 to coal for enhanced coalbed methane: experimental observations and numerical simulation. Int J Coal Geol. 2013;116–117:53–62. https://doi.org/10.1016/j.coal.2013.06.004.